Supporting Information

Zheng et al. 10.1073/pnas.1320815111

SI Materials and Methods

Tumor Xenograft Models. Approximately 6×10^6 M2 or A7 cells were implanted s.c. in 8- to 10-wk-old male SCID mice ($n = 6$). Mice were kept under standard conditions and had free access to food. Tumor size was measured every other day from day 7 after injection for 24 d. The animal studies were approved by the North Stockholm Ethical Committee for Care and Use of Laboratory Animals.

Whole-Mount Staining. The tumor vasculature was studied using whole-mount staining as previously described (1). The slides were stained with anti-CD31 (BD Pharmingen) and anti-NG2 antibody (Chemicon), followed by Alexa Fluor 555 and Alexa Fluor 488 antibodies (Invitrogen), respectively, to label endothelial cells and pericytes.

Yeast Two-Hybrid Screening. A GAL4-based system (2) (Matchmaker GAL4 two-hybrid system 3; Clontech) was used to screen a human T-cell cDNA library to identify previously unidentified proteins interacting with HIF-1α. The N-terminal 984-bp (amino acids 1–328) fragment of human hypoxia-inducible factor (HIF)-1α was cloned into pGBKT7, which was transformed into Y190 yeast strain, and no spontaneous transactivation was detected. Transformed yeast was expanded and mated with yeasts pretransformed with a human T-cell cDNA library (Clontech).

Cell Culture. M2, a human melanoma cell line (3) lacking both filamin A (FLNA) mRNA and protein, and its subline, A7 cell line (ATCC), a stably transfected M2 cell line expressing FLNA, were cultured in modified Eagle's medium (MEM). G418 (0.3 mg/mL) was added to the medium to maintain FLNA expression in A7 cells. NIH 3T3, HEK 293T, human osteosarcoma U2OS, HeLa, and COS-1 cells were cultured in DMEM. HEK 293A cells were maintained in a 1:1 mixture of DMEM and F-12 medium. All media were supplemented with 10% (vol/vol) FCS, 50 IU/mL penicillin, and 50 μg/mL streptomycin sulfate. Medium and other products for cell culture were purchased from Invitrogen. Cells were cultured at 37 °C under normoxic [21% (vol/vol) O_2] or hypoxic (1% O_2) conditions. The cells were exposed to hypoxia for 8 h before harvest unless it is specifically indicated.

Plasmid Constructs. To construct pFLAG/FLNA (ΔH1) encoding the H1 domain deletion mutant of FLNA, we first generated PCR fragment from pFLAG/FLNA containing FLNA residues 1336–1740 using primer pairs carrying restriction sites for PshA1 in the 5′ end and BssHII-XbaI in the 3′ end. The PCR fragment was inserted in frame into PshAI-XbaI–digested pFLAG/FLNA generating pFLAG/FLNA (1–1740). Another PCR fragment was amplified from pFLAG/FLNA containing residues 1778–2647 using primer pairs carrying restriction sites for BssHII in the 5′ end and stop codon/XbaI in the 3′ end. The PCR fragment was then inserted in frame into BssHII-XbaI–digested pFLAG/FLNA (1–1740). The inserts generated by PCR were completely sequenced using a DYEnamic sequencing kit (Amersham Biosciences). pFLAG/FLNA$^{16\text{-}24}$ encoding C-terminal FLNA repeats 16–24 was constructed by subcloning a BssHII-XbaI fragment containing FLNA amino acids 1778–2647 from pFLAG/FLNA(ΔH1) into EcoRI-XbaI-digested pFLAG-CMV-2 vector (Sigma), with the BssHI and EcoRi sites being previously filled in with the Klenow fragment of DNA polymerase I. pSV2-neo was purchased from Clontech. pCMX, pFLAG/FLNA, pcDNA3-HA/FLNA$^{20\text{-}24}$ encoding HA epitope-tagged C-terminal FLNA repeats 20–24, pFLAG/HIF-1α, pT81/HRE-luc, pCMX-GFP/HIF-1α, and pFLAG/mHIF-1α(1-390), pFLAG-GAL4/mHIF-1α(392-622), and pFLAG/mHIF-1α(531-822) have been described previously (4–10). The pFLAG-HIF-2α was a gift from Sakari Karttunen (Karolinska Institute, Stockholm).

Transient and Stable Transfections. Transient transfections in M2, A7, and 3T3 cells were performed using FuGENE 6 (Roche Molecular Biochemicals). In hypoxia-responsive element (HRE)-driven luciferase reporter assay, cells were cotransfected with 250 ng of HRE-driven luciferase reporter plasmid (pT81/HRE-luc) and 750 ng of pCMX. Twenty-four hours after transfection, the cells were exposed to either normoxia or hypoxia for 20 h and then lysed in cell culture lysis reagent (Promega). Luciferase activity was measured and normalized by protein concentration. In the analysis of subcellular distribution of GFP-fused HIF-1α, cells were transfected with 1.0 μg of expression plasmids. To detect the interaction between HA-FLNA$^{20\text{-}24}$ and HIF-1α or HIF-2α and to map the FLNA-interacting domains in HIF-1α, HEK 293A cells were cotransfected by 0.3 μg of pcDNA3-HA/FLNA$^{20\text{-}24}$ and 1.0 μg of FLAG-tagged expression plasmids for HIF-1α, HIF-2α, or HIF-1α deletion mutants using Lipofectamine (Invitrogen). All of the transfections were performed according to the manufacturer's instructions.

The stable cell lines were generated by cotransfecting 0.05 μg of pSV2-neo encoding anti-geneticin gene and 1.0 μg of FLAG-tagged expression plasmids for FLNA and its mutants into M2 cells, and positive clones were selected using 1 mg/mL geneticin.

RNA Interference Experiments. Negative control siRNA and siRNA duplex specific for FLNA with the DNA target sequence CAA CAC CAA GGA TGC AGG AGA were obtained from Qiagen. siRNA (100 nM) was transfected into A7 cells using Oligofectamine (Invitrogen) and into HEK 293T, HeLa, and U2OS cells using HiPerFect transfection reagent (Qiagen) according to the manufacturer's protocol. Forty-eight hours after transfection, the cells were cultured under normoxic or hypoxic conditions for 8 h before harvest.

Protein Extraction and Immunoprecipitation Assays. Protein extracts from tumors were made using TRIzol reagent (Life Technologies) according to the manufacturer's protocol. The preparation of whole-cell extracts using high-salt buffer and subcellular fractionation were performed as described before (11). To investigate the interaction of HA-FLNA$^{20\text{-}24}$ with HIF-1α or HIF-2α and to map the domains of HIF-1α that interact with HA-FLNA$^{20\text{-}24}$, whole-cell extracts were incubated overnight at 4 °C in BC180 buffer containing 50 mM Tris·HCl (pH 7.4), 180 mM NaCl, 0.2% Nonidet P-40, and 20% (vol/vol) glycerol under rotation with 50 μL Protein G-Sepharose slurry (Amersham Biosciences) preincubated with anti-FLAG M2 antibody. After three washes with Tris-buffered saline (TBS) buffer [50 mM Tris (pH 7.4), 150 mM NaCl] supplemented with 0.5% Triton X-100 and two washes with TBS buffer, the precipitated proteins were eluted by 0.5 mg/mL FLAG peptide (Sigma) in TBS buffer for 1.5 h at room temperature. To investigate the interaction of HIF-α with endogenous FLNA, transfected NIH 3T3 cells were lysed with a radioimmune precipitation buffer [10 mM Tris·HCl (pH 7.4), 150 mM NaCl, 5 mM EDTA, 1% Triton X-100, 0.1% SDS, and 1% sodium deoxycholate]. Precleared cell lysates were subjected to immunoprecipitation with anti-FLNA (Chemicon International) antibodies after absorption to protein G-Sepharose

beads. The eluted and immunoprecipitated proteins were analyzed by SDS/PAGE followed by immunoblotting assays.

Immunoblotting Assays. Immunoprecipitated proteins and protein from tumor xenografts, whole-cell extracts, and nuclear or cytosolic extracts were analyzed by immunoblotting assays as previously described (11). The anti-FLAG M2 (F3165, Sigma), anti-HA (sc-7392, Santa Cruz Biotechnology), anti-HIF-1α (ab6489, Abcam; or NB100-449, Novus Biologicals), anti-HIF-2α (NB100-132, Novus Biologicals), anti-FLNA (MAB1680 or MAB1678, Chemicon), anti-YY1 (sc-7341, Santa Cruz Biotechnology), and anti-β-actin (ab6276, Abcam) antibodies were used.

RNA Extraction and Quantitative RT-PCR. Total RNA from tumors were extracted using TRIzol reagent (Life Technologies) according to the manufacturer's protocol. RNA extraction from cell culture and quantitative RT-PCR were performed as described before (12). The primer sequences are as following. *VEGF-A*: 5′-ACT GAG GAG TCC AAC ATC AC-3′ and 5′-CTT TCT TTG GTC TGC ATT CAC-3′; *BNIP3*: 5′-GCA GAC ACC ACA AGA TAC C-3′ and 5′-ATC TTC CTC AGA CTG TGA GC-3′; *PGK1*: 5′-AGT CCT TAT GAG CCA CCT-3′ and 5′-CAG AAC ATC CTT GCC CAG-3′; *GLUT1*: 5′-CAG CAG CAA GAA GCT GAC-3′ and 5′-GGG CAT TGA TGA CTC CAG-3′; *GLUT3*: 5′-CAG GAG ATG AAA GAT GAG AGT G-3′ and 5′-AAT AGA ACA CAG CAT TGA TCC C-3′; *FLNA*: 5′-ACT GTT TCT AGC CTT CAG GAG-3′ and 5′-GCA CAG CAT ACT TAT CTT GGT C-3′; *β-actin*: 5′-AAG ATC AAG ATC ATT GCT CCT C-3′ and 5′-ATC TGC TGG AAG GTG GAC-3′. The expression of *β-actin* was used as an internal control. Experiments were performed at least three times in triplicates.

VEGF-A Secretion. Fifty microliters of supernatant from cell culture medium was used for the quantification of secreted VEGF-A protein using VEGF ELISA kit according to the manufacturer's instruction (Biosource International). Level of secreted VEGF-A was normalized to the total protein level. Experiments were performed at least three times in triplicates.

Visualization of Subcellular Localization of Fluorescent Proteins. The subcellular localization of fluorescent proteins in 4% (wt/vol) paraformaldehyde-fixed cells was analyzed using a laser scanning confocal microscope (LSM 510; Carl Zeiss) with 40× objectives at room temperature and quantified as described before (4, 11). Briefly, fluorescent cells were classified into five categories according to their subcellular localization: N, exclusively nuclear localization; N>C, predominantly nuclear localization; N=C, equal distribution in both cytoplasm and nucleus; N<C, predominantly cytoplasmic localization; and C, exclusively cytoplasmic localization. On average, 250 cells were evaluated on each coverslip. The images were acquired and processed using Zeiss LSM Image Browser.

ChIP Assay. The ChIP assay was performed as previously described (10). Briefly, M2, A7, and COS1 cells were cultured under normoxic or hypoxic conditions for 8 h. The soluble chromatin was immunoprecipitated using anti-HIF-1α (ab2185, Abcam), anti-C terminus of FLNA (Santa Cruz Biotechnology, sc-28284, epitope: amino acids 2348–2647), or anti-human IgG (Jackson ImmunoResearch Laboratories, 309-005-003) antibody. The immunoprecipitated DNA fragments were then purified and followed by PCR analysis to amplify the *VEGF-A* and *PGK1* promoter region spanning HRE consensus. The primer sequences are as follows: *VEGF-A* promoter: 5′-CCC TTT GGG TTT TGC CAG A-3′ and 5′-AAC GGG AAG CTG TGT GGT TC-3′; *PGK1* promoter: 5′-TCC GTT CGC AGC GTC ACC-3′ and 5′-CGC TGC CAT TGC TCC CTG-3′.

Bioinformatic Analysis of Oncomine Cancer Gene Microarray Database. We analyzed datasets from the Oncomine database (Compendia Biosciences; www.oncomine.org) to compare the FLNA mRNA expression between cancer and normal tissues (either disease-free normal and/or normal adjacent tissues). These datasets provide fold-change data for gene expression, with *P* values calculated by *t* tests (13).

Statistical Analysis. Two-tailed Student *t* test was used to analyze the difference between two samples. The data are shown as mean ± SD of at least three independent experiments. The difference was considered significant if $P < 0.05$.

1. Nissen LJ, et al. (2007) Angiogenic factors FGF2 and PDGF-BB synergistically promote murine tumor neovascularization and metastasis. *J Clin Invest* 117(10):2766–2777.
2. Fields S, Song O (1989) A novel genetic system to detect protein-protein interactions. *Nature* 340(6230):245–246.
3. Cunningham CC, et al. (1992) Actin-binding protein requirement for cortical stability and efficient locomotion. *Science* 255(5042):325–327.
4. Kallio PJ, et al. (1998) Signal transduction in hypoxic cells: Inducible nuclear translocation and recruitment of the CBP/p300 coactivator by the hypoxia-inducible factor-1alpha. *EMBO J* 17(22):6573–6586.
5. Ruas JL, Poellinger L, Pereira T (2002) Functional analysis of hypoxia-inducible factor-1 alpha-mediated transactivation. Identification of amino acid residues critical for transcriptional activation and/or interaction with CREB-binding protein. *J Biol Chem* 277(41):38723–38730.
6. Tanimoto K, Makino Y, Pereira T, Poellinger L (2000) Mechanism of regulation of the hypoxia-inducible factor-1 alpha by the von Hippel-Lindau tumor suppressor protein. *EMBO J* 19(16):4298–4309.
7. Umesono K, Murakami KK, Thompson CC, Evans RM (1991) Direct repeats as selective response elements for the thyroid hormone, retinoic acid, and vitamin D3 receptors. *Cell* 65(7):1255–1266.
8. Sasaki A, Masuda Y, Ohta Y, Ikeda K, Watanabe K (2001) Filamin associates with Smads and regulates transforming growth factor-beta signaling. *J Biol Chem* 276(21): 17871–17877.
9. Chen D, Li M, Luo J, Gu W (2003) Direct interactions between HIF-1 alpha and Mdm2 modulate p53 function. *J Biol Chem* 278(16):13595–13598.
10. Gustafsson MV, et al. (2005) Hypoxia requires notch signaling to maintain the undifferentiated cell state. *Dev Cell* 9(5):617–628.
11. Zheng X, et al. (2006) Cell-type-specific regulation of degradation of hypoxia-inducible factor 1 alpha: Role of subcellular compartmentalization. *Mol Cell Biol* 26(12):4628–4641.
12. Zheng X, et al. (2012) Acute hypoxia induces apoptosis of pancreatic β-cell by activation of the unfolded protein response and upregulation of CHOP. *Cell Death Dis* 3:e322.
13. Rhodes DR, et al. (2007) Oncomine 3.0: genes, pathways, and networks in a collection of 18,000 cancer gene expression profiles. *Neoplasia* 9(2):166–180.

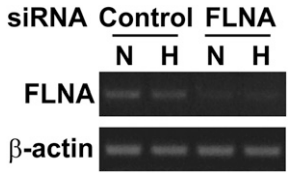

Fig. S1. Related to Fig. 2. FLNA mRNA level is down-regulated by siRNA targeting FLNA in A7 cells. A7 cells were transfected with a negative control siRNA (Control) or an siRNA targeting FLNA (FLNA). Cells were cultured under normoxic (N) or hypoxic (8 h) (H) conditions.

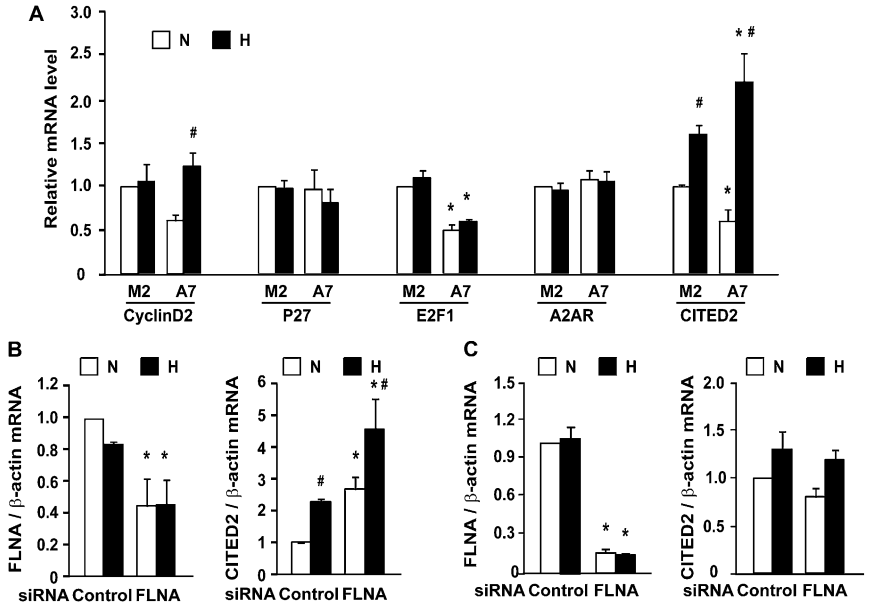

Fig. S2. Related to Fig. 2. Expression of HIF-2α target genes is not affected by FLNA. (*A*) The relative mRNA expression levels of HIF-2α target genes in M2 and A7 cells cultured in normoxia (N) or 8 h hypoxia (H) were analyzed using quantitative RT-PCR. $^{*}P < 0.05$ compared with corresponding samples of M2 cells; $^{\#}P < 0.05$ compared with normoxia. (*B* and *C*) Silencing of FLNA does not inhibit CITED2 gene expression. Relative mRNA expression of FLNA and CITED2 in A7 cells (*B*) and HEK 293T (*C*) cells were analyzed using quantitative RT-PCR. Data are shown as mean ± SD of at least three independent experiments. $^{*}P < 0.05$ compared with corresponding samples transfected with control siRNA; $^{\#}P < 0.05$ compared with normoxia.

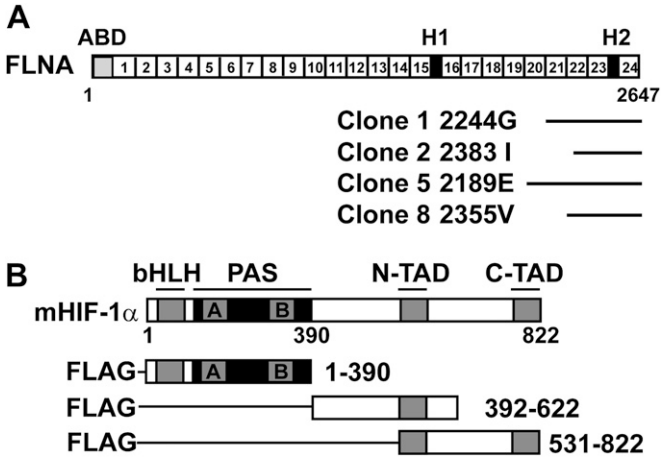

Fig. S3. Related to Fig. 3. (*A*) Schematic representation of the monomeric FLNA structure and the clones identified to interact with HIF-1α. Indicated are the actin-binding domain (ABD), hinge-1 and -2 (H1 and H2) regions, and the 24 Ig-like rod-domain repeats (approximately 96 amino acids in each). (*B*) Schematic representation of HIF-1α deletion mutants used in Fig. 3*C*. The basic helix–loop–helix (bHLH), Per-Arnt-Sim domain (PAS), N-terminal transactivation (N-TAD), and C-terminal transactivation (C-TAD) domains are indicated.

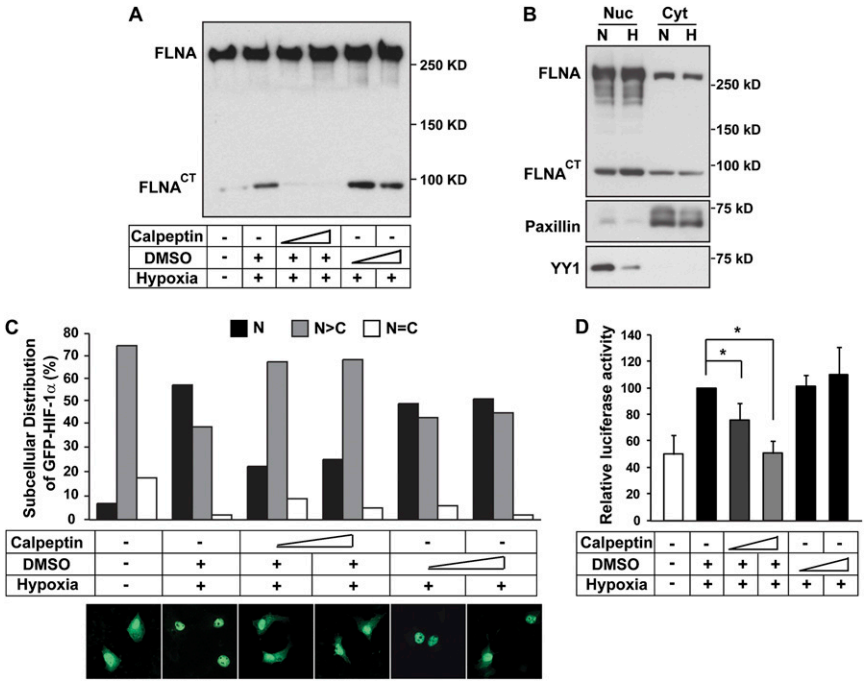

Fig. S4. Related to Fig. 4. Calpain-dependent cleavage of FLNA is essential for the regulation of HIF-1α localization and function in COS-1 cells. (*A*) Hypoxia enhances calpain-dependent cleavage of FLNA in COS-1 cells. COS-1 cells were cultured in normoxia or hypoxia and treated with either calpain inhibitor calpeptin (50 and 100 μM) or DMSO as control for 8 h. The expression of full-length FLNA and FLNA^{CT} were detected by immunoblott analysis using an antibody against the C terminus of FLNA. (*B*) FLNA^{CT} is present in both nuclear and cytoplasmic cellular fractions. Expression of full-length FLNA and FLNA^{CT} was detected by using an antibody against the C terminus of FLNA. Expression of paxillin and YY1 is also shown as nuclear and cytoplasmic protein markers, respectively. (*C*) Inhibition of FLNA cleavage by calpeptin impairs GFP-HIF-1α nuclear accumulation. Subcellular localization of GFP-fused HIF-1α in M2 and A7 cells cultured in normoxia or hypoxia and treated with calpeptin or DMSO as above. Representative images are shown. Quantitative evaluation are presented as percentage of cells belonging to the categories N (exclusively nuclear localization), N>C (predominantly nuclear localization), and N=C (equal distribution in both cytoplasm and nucleus). (*D*) Inhibition of FLNA cleavage by calpeptin decreases HIF-1α transactivation activity. COS1 cells were cultured and treated as above. Relative HRE-driven luciferase activity is shown. The value of hypoxia-treated cells is set to 100. Data are shown as mean ± SD of at least three independent experiments. *$P < 0.05$.

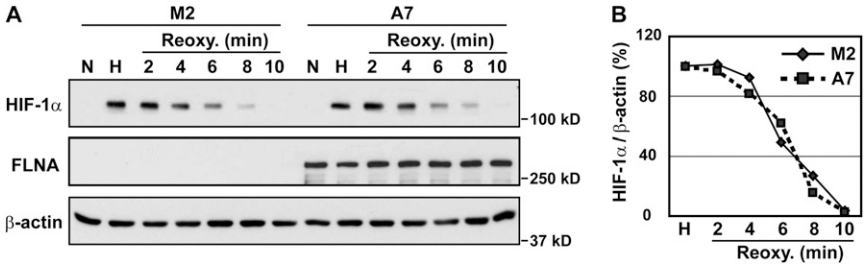

Fig. S5. Half-life of HIF-1α is not affected by FLNA. M2 and A7 cells were cultured in normoxia (N) or hypoxia (H) for 8 h. After hypoxia treatment, cells were exposed to 2, 4, 6, 8, or 10 min of reoxygenation (Reoxy.). (*A*) Immunoblotting analysis for endogenous HIF-1α, FLNA, and β-actin. (*B*) Quantification of endogenous HIF-1α protein levels normalized by β-actin expression levels.

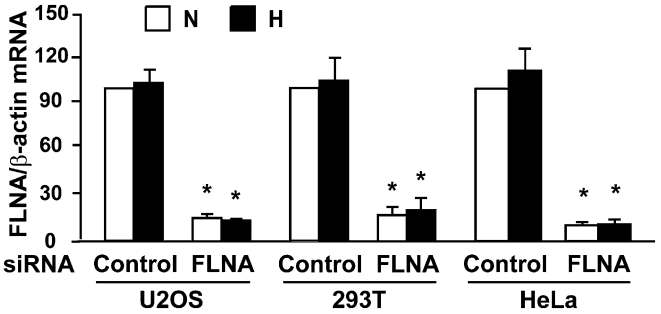

Fig. S6. Related to Fig. 5. FLNA mRNA level is down-regulated by siRNA targeting FLNA in U2OS, 293T, and HeLa cells. Cells were transfected with a negative control siRNA (Control) or an siRNA targeting FLNA (FLNA), and cultured under normoxic (N) or hypoxic (8 h) (H) conditions. The relative mRNA level of FLNA was detected using quantitative RT-PCR. Data are shown as mean ± SD of at least three independent experiments. *$P < 0.05$.

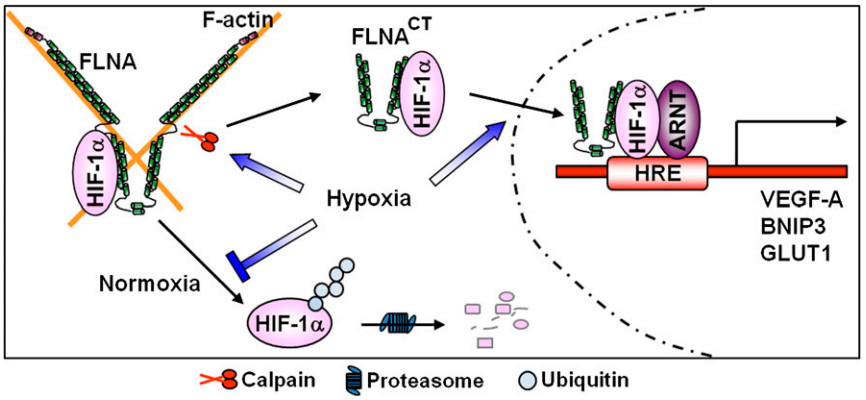

Fig. S7. Schematic illustration of the regulation of HIF-1α function by FLNA. FLNA interacts with HIF-1α but not HIF-2α in the cytoplasm. Calpain protease activity that is increased at hypoxia cleaves FLNA releasing the $FLNA^{CT}$, which translocates to the nucleus together with HIF-1α. As part of the HIF-1α transcriptional complex, $FLNA^{CT}$ binds to HRE-containing promoter regions of HIF-1α target genes. Thus, $FLNA^{CT}$ increases the HIF-1α transactivation function by facilitating HIF-1α translocation to the nucleus and/or nuclear retention and/or by working as a transcriptional coactivator.

Table S1. Cancers that have increased FLNA mRNA level compared with normal tissues

Cancer type	# Total	# Upp	# No change	# Down	Upp, *P* value	Upp, fold change
Brain and central nervous system cancer						
Glioblastoma	6	4	1	1	(4.14E−29) to (0.027)	(1.301) to (4.649)
Anaplastic oligodendroglioma	1	1	0	0	7.66E−07	2.231
Astrocytoma	1	1	0	0	5.50E−06	4.509
Anaplastic astrocytoma	1	1	0	0	8.00E−6	2.172
Cervical cancer	1	1	0	0	0.002	1.431
Colorectal carcinoma	4	3	1	0	(1.28E−04) to (2.18E−06)	(1.379) to (1.666)
Gastric adenocarcinoma	6	3	3	0	(5.43E−07) to (0.005)	(2.035) to (2.27)
Head-and-neck cancer						
Salivary gland adenoid cystic carcinoma	1	1	0	0	4.05E−08	4.612
Thyroid gland carcinoma	3	3	0	0	(2.28E−04) to (7.28E−04)	(1.264) to (1.492)
Head and neck carcinoma	4	4	0	0	(2.34E−06) to (1.80E−02)	(1.408) to (2.747)
Leukemia/lymphoma						
Mantle cell lymphoma	1	1	0	0	3.96E−06	3.184
Adult T-cell leukemia/lymphoma	2	2	0	0	(9.12E−06) to (0.012)	(1.709) to (1.767)
Myeloid leukemia	2	2	0	0	(2.29E−05) to (0.006)	(1.129) to (1.248)
Hairy cell leukemia	1	1	0	0	3.14E−07	3.328
Oral carcinoma	9	5	4	0	(7.80E−09) to (0.034)	(1.187) to (2.932)
Clear cell renal cell carcinoma	7	7	0	0	(6.75E−07) to (3.1E−02)	(1.294) to (2.37)
Pancreatic adenocarcinoma	6	4	1	1	(3.31E−10) to (4.00E−02)	(1.374) to (4.623)
Leiomyosarcoma	3	2	1	0	(4.75E−19) to (1.84E−05)	(5.967) to (6.276)
Seminoma	5	5	0	0	(8.00E−11) to (1.24E−06)	(2.915) to (3.848)

#Total, number of total studies performed for each type of cancer; # Upp, number of total studies showing increased *FLNA* expression in the indicated cancer type; # No change, number of total studies showing no change in *FLNA* expression in the indicated cancer type; # Down, number of total studies showing decreased *FLNA* expression in the indicated cancer type.

Table S2. Cancers that have decreased FLNA mRNA level compared with normal tissues

Cancer type	# Total	# Upp	# No change	# Down	Down, *P* value	Down, fold change
Superficial bladder cancer	3	0	1	2	(2.39E−21) to (6.84E−05)	(2.407) to (11.472)
Brain and central nervous system cancer						
Oligodendroglioma	1	0	0	1	1.00E−03	2.365
Anaplastic oligoastrocytoma	1	0	0	1	2.94E−04	1.878
Invasive breast carcinoma stroma	1	0	0	1	5.92E−06	4.152
Colorectal adenocarcinoma	14	0	4	10	(1.25E−7) to (0.029)	(1.208) to (3.073)
Leukemia/lymphoma						
B-cell acute lymphoblastic leukemia	3	0	1	2	(1.22E−23) to (1.15E−22)	(1.863) to (2.035)
Acute myeloid leukemia	2	0	0	1	2.00E−02	2.334
Follicular lymphoma	2	0	0	2	(2.00E−03) to (5.00E−03)	(1.74) to (2.006)
Lung cancer						
Lung adenocarcinoma	7	0	1	6	(1.35E−05) to (2.00E−03)	(1.252) to (3.641)
Small cell lung carcinoma	2	0	1	1	4.47E−04	4.376
Lung carcinoid tumor	1	0	0	1	7.63E−10	28.733
Multiple myeloma	1	0	0	1	3.16E−05	1.72
Prostate carcinoma	12	0	3	9	(8.61E−11) to (0.033)	(1.437) to (2.778)
Parathyroid cancer						
Parathyroid gland adenoma	1	0	0	1	0.003	1.536
Parathyroid hyperplasia	1	0	0	1	0.008	1.433
Nonfamilial multiple gland neoplasia	1	0	0	1	0.006	1.459

#Total, number of total studies performed for each type of cancer; # Upp, number of total studies showing increased *FLNA* expression in the indicated cancer type; # No change, number of total studies showing no change in *FLNA* expression in the indicated cancer type; # Down, number of total studies showing decreased *FLNA* expression in the indicated cancer type.